


# Ratiometric Detection of Mitochondrial Thiols with a Two-Photon Fluorescent Probe

Chang Su Lim,<sup>†</sup> Goutam Masanta,<sup>‡</sup> Hyung Joong Kim,<sup>§</sup> Ji Hee Han,<sup>†</sup> Hwan Myung Kim,<sup>\*,‡,§</sup> and Bong Rae Cho<sup>\*,†</sup>

<sup>†</sup>Department of Chemistry, Korea University, 1-Anamdong, Seoul 136-701, Korea

<sup>‡</sup>Molecular Science & Technology Research Center, <sup>§</sup>Division of Energy Systems Research, Ajou University, Suwon 443-749, Korea

 Supporting Information

**ABSTRACT:** We report a ratiometric two-photon probe (SSH-Mito) for mitochondrial thiols. This probe shows a marked blue-to-yellow emission color change in response to RSH, a significant two-photon cross section, good mitochondrial thiol selectivity, low cytotoxicity, and insensitivity to pH over the biologically relevant pH range, allowing the direct visualization of RSH levels in live cells as well as in living tissues at 90–190  $\mu\text{m}$  depth without interference from other biologically relevant species through the use of two-photon microscopy.

Intracellular thiols such as cysteine (Cys), homocysteine (Hcy), and glutathione (GSH) play vital roles in biology.<sup>1</sup> They maintain higher-order structures of proteins and control redox homeostasis through the equilibrium between thiols (RSH) and disulfides (RSSR).<sup>2</sup> In mitochondria, a primary site of oxygen consumption and the major source of reactive oxygen species (ROS), GSH plays a key role in maintaining the redox environment to avoid or repair oxidative damage leading to dysfunction and cell death.<sup>3</sup> Mitochondrial GSH (mGSH) exists predominantly in the reduced form, with a GSH:GSSG ratio of  $>100:1$ .<sup>4</sup> An increase in the GSSG-to-GSH ratio is considered to be indicative of oxidative stress conditions.<sup>5</sup> To understand the roles of RSH in biology, it is crucial to monitor RSH at the cell, tissue, and organism level. For this purpose, a variety of fluorescent probes for RSH, derived from fluorescein, rhodamine, or green fluorescent protein (GFP) as the fluorophore and functional groups that react with RSH, have been developed.<sup>6</sup> However, most of these probes have been evaluated using one-photon microscopy (OPM) and require relatively short excitation wavelengths ( $<525$  nm), limiting their use in deep-tissue imaging because of the shallow penetration depth ( $<80$   $\mu\text{m}$ ). Moreover, although mitochondrial-targeted reagents for thiols have been developed,<sup>7</sup> no targetable fluorescent probe for mitochondrial RSH has been reported to date.

To detect RSH deep inside live tissues, it is crucial to use two-photon microscopy (TPM), a new technique that utilizes two photons of lower energy for excitation. TPM offers a number of advantages over OPM, including increased penetration depth ( $>500$   $\mu\text{m}$ ), localized excitation, and prolonged observation time.<sup>8,9</sup> Recently, we reported a two-photon (TP) turn-on probe, ASS, that can detect thiols in live cells and intact tissues by TPM.<sup>10</sup> However, its turn-on responses can vary depending on

the experimental conditions such as incident laser power and/or probe concentration, making it unsuitable for quantitative measurements. Therefore, there is a need to develop a TP probe for mitochondrial RSH.

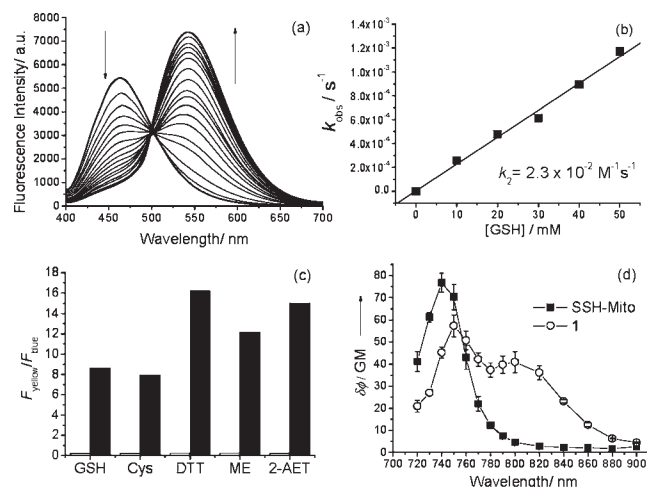
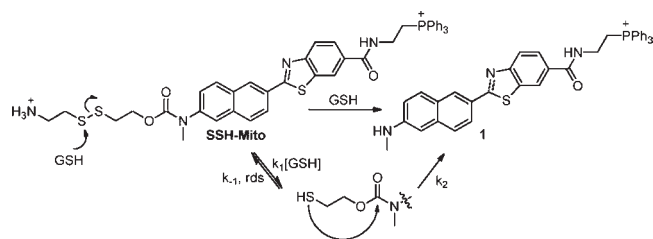
In this work, we have developed a ratiometric TP probe for mitochondrial thiols (SSH-Mito, Scheme 1) derived from 6-(benzo[*d*]thiazol-2'-yl)-2-(*N,N*-dimethylamino)naphthalene (BT DAN) as the reporter, a disulfide group as the thiol reaction site, and triphenylphosphonium salt (TPP) as the mitochondrial-targeting site. BT DAN has been successfully utilized in the TP probe for  $\text{Zn}^{2+}$  (SZn-Mito),<sup>11</sup> while disulfide is a well-known receptor for thiols<sup>6e,12</sup> and TPP is an effective mitochondrial-targeting site.<sup>13,14</sup> The disulfide bond and TPP are separated as far as possible to minimize the interactions between them. Herein we report that SSH-Mito can ratiometrically detect mitochondrial RSH in live cells and intact tissues at depths of  $>100$   $\mu\text{m}$  by TPM.

The preparation of SSH-Mito is described in the Supporting Information (SI). Its solubility as determined by the fluorescence method is  $5$   $\mu\text{M}$  in MOPS buffer ( $[\text{MOPS}] = 30$  mM,  $100$  mM KCl, pH 7.4), which is sufficient to stain cells (Figure S1 in the SI).<sup>15</sup> Under these conditions, SSH-Mito and **1** exhibit absorption maxima ( $\lambda_{\text{abs}}$ ) at  $338$  nm ( $\epsilon = 20\,500$   $\text{M}^{-1}$   $\text{cm}^{-1}$ ) and  $383$  nm ( $\epsilon = 15\,000$   $\text{M}^{-1}$   $\text{cm}^{-1}$ ) and fluorescence maxima ( $\lambda_{\text{fl}}$ ) at  $462$  nm ( $\Phi = 0.82$ ) and  $545$  nm ( $\Phi = 0.12$ ), respectively (Table S1 in the SI). The larger Stokes shift observed in **1** relative to SSH-Mito can be attributed to the greater stabilization of the charge-transfer excited state in the former, which contains a stronger electron-donating group.

The reaction between SSH-Mito and GSH produces **1** as the only product, as monitored by emission spectra (Figure 1a) and LC–MS analysis (Figure S3). The emission spectra of a  $5$   $\mu\text{M}$  solution of SSH-Mito treated with  $10$  mM GSH in MOPS buffer increased gradually at  $545$  nm with a concomitant decrease at  $462$  nm. This process followed first-order kinetics with  $k_{\text{obs}} = 3.0 \times 10^{-4}$   $\text{s}^{-1}$ , which was identical to that measured for the TP process (Figure S2). Moreover, the plot of  $k_{\text{obs}}$  versus  $[\text{GSH}]$  was a straight line passing through the origin. This indicates that the reaction is second-order overall, first-order with respect to SSH-Mito and first-order with respect to GSH, with  $k_2 = 2.3 \times 10^{-2}$   $\text{M}^{-1}$   $\text{s}^{-1}$  (Figure 1b). A nearly identical value was reported for the reaction of ASS with 2-aminoethanethiol (2-AET).<sup>10</sup> These results can most reasonably be attributed to rate-limiting

Received: June 2, 2011

Published: June 30, 2011

**Scheme 1. Structures of SSH-Mito and 1 and the Mechanism of GSH-Induced Reduction of SSH-Mito**


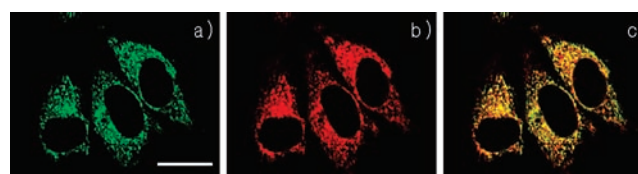
**Figure 1.** (a) One-photon fluorescence response as a function of time for the reaction of SSH-Mito ( $5 \mu M$ ) with GSH (10 mM) in MOPS buffer (30 mM, pH 7.4). (b) Plot of  $k_{obs}$  vs concentration of GSH. (c) Fluorescence responses of SSH-Mito toward GSH, Cys, DTT, 2-ME, and 2-AET. The white and black bars represent the integrated fluorescence ratios  $F_{yellow}/F_{blue}$  of SSH-Mito before and 2 h after addition of the thiols, respectively. (d) Two-photon action spectra of SSH-Mito and 1 in MOPS buffer.

attack of GSH on the disulfide bond followed by cleavage of the C–N bond to afford 1 (Scheme 1).

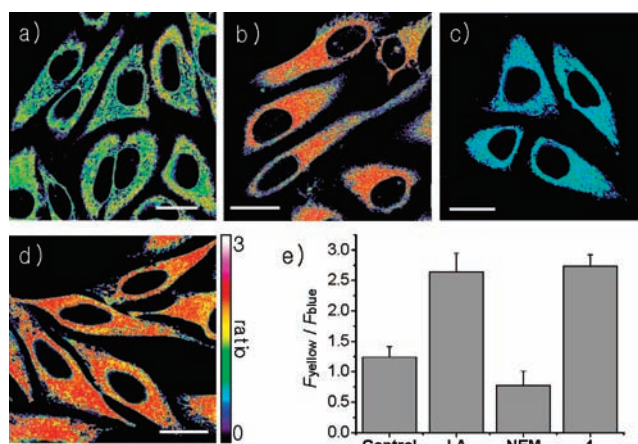
SSH-Mito exhibits a strong response toward thiols, including GSH, Cys, dithiothreitol (DTT), 2-mercaptoethanol (2-ME), and 2-AET, and negligible responses toward amino acids without thiol groups (Glu, Ser, Val, Met, Ala, Ile), metal ions ( $Na^+$ ,  $K^+$ ,  $Ca^{2+}$ ,  $Mg^{2+}$ ,  $Zn^{2+}$ ), and  $H_2O_2$  (Figure 1c and Figure S4) and is pH insensitive at biologically relevant pH (Figure S5). Furthermore,  $F_{yellow}/F_{blue}$ , the ratio of the intensities at 425–475 nm ( $F_{blue}$ ) and 525–575 nm ( $F_{yellow}$ ), increased by 42–77-fold (Figure 1c). These results establish that SSH-Mito can serve as a fluorescent ratiometric probe for intracellular thiols without interference from other biologically relevant analytes and pH.

The TP action spectra of SSH-Mito and 1 in MOPS buffer (pH 7.4) indicate  $\Phi\delta_{max}$  values of 80 and 55 GM at 740 and 750 nm, respectively, which are comparable to those of existing TP probes (Figure 1d).<sup>9</sup> This predicts that staining of living specimens with SSH-Mito should produce bright TPM images, as was observed (see below).

We next sought to apply SSH-Mito as a TP probe for detecting mitochondrial RSH in cellular environments. To confirm whether SSH-Mito can specifically stain the mitochondria, a colocalization



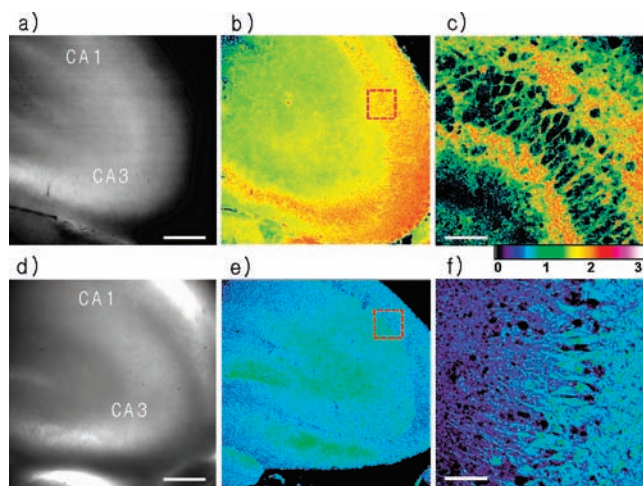
**Figure 2.** (a) TPM and (b) OPM images of HeLa cells colabeled with (a) SSH-Mito ( $5 \mu M$ ) and (b) MitoTracker Red FM ( $5 \mu M$ ) for 30 min at  $37^\circ C$ . (c) Co-localized image. The wavelengths for one- and two-photon excitation were 514 and 740 nm, respectively, and the emission was collected at 425–575 nm (SSH-Mito) and 600–700 nm (MitoTracker Red FM). Scale bar,  $30 \mu m$ . Cells shown are representative images from replicate experiments ( $n = 5$ ).



**Figure 3.** (a–d) Pseudocolored ratiometric TPM images ( $F_{yellow}/F_{blue}$ ) of HeLa cells incubated with  $5 \mu M$  (a) SSH-Mito and (d) 1 and cells pretreated with (b) lipoic acid (500  $\mu M$ ) for 1 day and (c) NEM (100  $\mu M$ ) for 30 min before labeling with SSH-Mito. (e) Average  $F_{yellow}/F_{blue}$  intensity ratios in (a–d). Images were acquired using 740 nm excitation and fluorescent emission windows of 425–475 nm (blue) and 525–575 nm (yellow). Scale bar,  $20 \mu m$ . Cells shown are representative images from replicate experiments ( $n = 5$ ).

experiment was conducted with the HeLa cells costained with SSH-Mito and MitoTracker Red, a well-known one-photon fluorescent probe for mitochondria.<sup>16</sup> The TPM image merged well with the OPM image of mitochondria (Figure 2c). Moreover, the Pearson's colocalization coefficient (calculated using Autoquant X2 software) of SSH-Mito with MitoTracker Red was 0.85, indicating that SSH-Mito exists predominantly in mitochondria.

Upon TP excitation at 740 nm, the ratio image of the HeLa cells labeled with SSH-Mito constructed from two collection windows gave an average emission ratio of 1.24 (Figure 3a,e and Figure S6). More importantly, SSH-Mito was responsive to the changes in the thiol concentration: the  $F_{yellow}/F_{blue}$  ratio increased to 2.64 when the cells were preincubated for 1 day with  $\alpha$ -lipoic acid (Figure 3b), which increases GSH production,<sup>17</sup> and the value was nearly identical to that obtained with 1 (2.73, Figure 3d). The  $F_{yellow}/F_{blue}$  ratio also decreased to 0.77 upon treatment with *N*-ethylmaleimide (NEM) (Figure 3c), a well-known thiol-blocking agent.<sup>18</sup> Further, SSH-Mito was found to be nontoxic to cells during the imaging experiments, as determined using a CCK-8 kit (Figure S7). These findings demonstrate that SSH-Mito is capable of detecting mitochondrial thiols in live cells.



**Figure 4.** Images of a rat hippocampal slice stained with 20  $\mu\text{M}$  SSH-Mito for 2 h. (a, d) Bright-field images of the CA1 and CA3 regions. (b, e) Ratiometric TPM images of a fresh rat hippocampal slices that were (b) not treated and (e) pretreated with NEM (100  $\mu\text{M}$ ) for 30 min before labeling with SSH-Mito. Ten ratiometric TPM images were accumulated along the z direction at depths of 90–190  $\mu\text{m}$  with 10 $\times$  magnification. (c, f) Enlarged images of the red boxes in (b) and (e) at a depth of 120  $\mu\text{m}$  with 40 $\times$  magnification. The TP fluorescence emission was collected in two channels (blue = 425–475 nm, yellow = 525–575 nm) upon excitation at 740 nm with a femtosecond pulse. Scale bars: (a, d) 300  $\mu\text{m}$ ; (c, f) 75  $\mu\text{m}$ .

We further investigated the utility of this probe in tissue imaging. The bright-field image of a part of a fresh rat hippocampal slice reveals the CA1 and CA3 regions (Figure 4a,d). As the structure of the brain tissue is known to be inhomogeneous throughout its entire depth, we accumulated 10 TPM images from the two collection windows at depths of 90–190  $\mu\text{m}$  to visualize the overall thiol distribution. They revealed that thiols are more or less evenly distributed in both the CA1 and CA3 regions (Figure 4b). Moreover, the image at a higher magnification clearly shows the thiol distribution in the individual cells in the CA1 region with an average emission ratio of 1.66 at a depth of 120  $\mu\text{m}$  (Figure 4c). When the tissue was treated with 100  $\mu\text{M}$  NEM for 30 min, the ratio decreased to 0.85 (Figure 4f). It is worth noting that the changes in the emission ratios measured deep inside the tissue slice are comparable to those in the cells. Furthermore, the TPM images at depths of 90, 120, 160, and 190  $\mu\text{m}$  show the thiol distribution in each  $xy$  plane along the  $z$  direction (Figure S8). These findings demonstrate that SSH-Mito is capable of detecting thiols at depths of a 90–190  $\mu\text{m}$  in live tissues using TPM.

To conclude, we have developed a new ratiometric TP probe, SSH-Mito, which shows a significant TP cross section, a marked blue-to-yellow emission color change in response to RSH, good mitochondrial thiol selectivity, low cytotoxicity, and insensitivity to pH over the biologically relevant pH range. This new probe can visualize mitochondrial RSH levels in live cells as well as in living tissues at depths of 90–190  $\mu\text{m}$  without interference from other biologically relevant species.

## ■ ASSOCIATED CONTENT

**S Supporting Information.** Synthesis and photophysical properties of SSH-Mito, cell culture, and two-photon imaging.

This material is available free of charge via the Internet at <http://pubs.acs.org>.

## ■ AUTHOR INFORMATION

### Corresponding Author

kimhm@ajou.ac.kr; chobr@korea.ac.kr

## ■ ACKNOWLEDGMENT

This work was supported by grants from the National Research Foundation (NRF) funded by the Korean Government (2011-0004321 and 2010-0018921) and the Priority Research Centers Program through the NRF funded by the Ministry of Education, Science and Technology (2010-0028294 and 2010-0020209) and by an Ajou University Research Fellowship of 2010. C.S.L., H.J.K., and J.H.H. were supported by BK21 Scholarships.

## ■ REFERENCES

- (1) (a) Wood, Z. A.; Schröder, E.; Harris, J. R.; Poole, L. B. *Trends Biochem. Sci.* **2003**, *28*, 32. (b) *Homocysteine in Health and Disease*; Carmel, R., Jacobsen, D. W., Eds.; Cambridge University Press: Cambridge, U.K., 2001. (c) Dalton, T. P.; Shertzer, H. G.; Puga, A. *Annu. Rev. Pharmacol. Toxicol.* **1999**, *39*, 67.
- (2) Kizek, R.; Vacek, J.; Trnková, L.; Jelen, F. *Bioelectrochemistry* **2004**, *63*, 19.
- (3) Mari, M.; Morales, A.; Colell, A.; García-Ruiz, C.; Fernández-Checa, J. C. *Antioxid. Redox Signaling* **2009**, *11*, 2685.
- (4) Schafer, F. Q.; Buettner, G. R. *Free Radical Biol. Med.* **2001**, *30*, 1191.
- (5) Russell, J.; Rabenstein, D. L. *Anal. Biochem.* **1996**, *242*, 136.
- (6) (a) Long, L.; Lin, W.; Chen, B.; Gao, W.; Yuan, L. *Chem. Commun.* **2011**, *47*, 893. (b) Chen, X.; Ko, S.-K.; Kim, M. J.; Shin, I.; Yoon, J. *Chem. Commun.* **2010**, *46*, 2751. (c) Lin, W.; Yuan, L.; Cao, Z.; Feng, Y.; Long, L. *Chem.—Eur. J.* **2009**, *15*, 5096. (d) Li, H.; Fan, J.; Wang, J.; Tian, M.; Du, J.; Sun, S.; Sun, P.; Peng, X. *Chem. Commun.* **2009**, 5904. (e) Pires, M. M.; Chmielewski, J. *Org. Lett.* **2008**, *10*, 837. (f) Shibata, A.; Furukawa, K.; Abe, H.; Tsuneda, S.; Ito, Y. *Bioorg. Med. Chem. Lett.* **2008**, *18*, 2246. (g) Sreejith, S.; Divya, K. P.; Ajayaghosh, A. *Angew. Chem., Int. Ed.* **2008**, *47*, 7883. (h) Fujikawa, Y.; Urano, Y.; Komatsu, T.; Hanaoka, K.; Kojima, H.; Terai, T.; Inoue, H.; Nagano, T. *J. Am. Chem. Soc.* **2008**, *130*, 14533. (i) Ahn, Y.-H.; Lee, J.-S.; Chang, Y.-T. *J. Am. Chem. Soc.* **2007**, *129*, 4510. (j) Zhang, M.; Yu, M.; Li, F.; Zhu, M.; Li, M.; Gao, Y.; Li, L.; Liu, Z.; Zhang, J.; Zhang, D.; Yi, T.; Huang, C. *J. Am. Chem. Soc.* **2007**, *129*, 10322. (k) Tang, B.; Xing, Y.; Li, P.; Zhang, N.; Yu, F.; Yang, G. *J. Am. Chem. Soc.* **2007**, *129*, 11666. (l) Chen, H.; Zhao, Q.; Wu, Y.; Li, F.; Yang, H.; Yi, T.; Huang, C. *Inorg. Chem.* **2007**, *46*, 11075. (m) Püllela, P. K.; Chiku, T.; Carvan, M. J.; Sem, D. S. *Anal. Biochem.* **2006**, *352*, 265. (n) Wang, W.; Rusin, O.; Xu, X.; Kim, K. K.; Escobedo, J. O.; Fakayode, S. O.; Kristin, A.; Fletcher, K. A.; Lowry, M.; Schowalter, C. M.; Lawrence, C. M.; Fronczek, F. R.; Warner, I. M.; Strongin, R. M. *J. Am. Chem. Soc.* **2005**, *127*, 15949.
- (7) (a) Coulter, C. V.; Kelso, G. F.; Lin, T. K.; Smith, R. A.; Murphy, M. P. *Free Radical Biol. Med.* **2000**, *28*, 1547. (b) James, A. M.; Cocheme, H. M.; Murphy, M. P. *Mech. Ageing Dev.* **2005**, *126*, 982.
- (8) (a) Helmchen, F.; Denk, W. *Nat. Methods* **2005**, *2*, 932. (b) Zipfel, W. R.; Williams, R. M.; Webb, W. W. *Nat. Biotechnol.* **2003**, *21*, 1369.
- (9) (a) Kim, H. M.; Cho, B. R. *Acc. Chem. Res.* **2009**, *42*, 863. (b) Kim, H. M.; Cho, B. R. *Chem.—Asian J.* **2011**, *6*, 58.
- (10) Lee, J. H.; Lim, C. S.; Tian, Y. S.; Han, J. H.; Cho, B. R. *J. Am. Chem. Soc.* **2010**, *132*, 1216.
- (11) Masanta, G.; Lim, C. S.; Kim, H. J.; Han, J. H.; Kim, H. M.; Cho, B. R. *J. Am. Chem. Soc.* **2011**, *133*, 5698.

(12) Zhu, B.; Zhang, X.; Li, Y.; Wang, P.; Zhang, H.; Zhuang, X. *Chem. Commun.* **2010**, 46, 5710.

(13) (a) Murphy, M. P.; Smith, R. A. *Annu. Rev. Pharmacol. Toxicol.* **2007**, 47, 629. (b) Yousif, L. F.; Stewart, K. M.; Kelley, S. O. *ChemBioChem* **2009**, 10, 1939.

(14) (a) Dickinson, B. C.; Chang, C. J. *J. Am. Chem. Soc.* **2008**, 130, 9638. (b) Dickinson, B. C.; Srikun, D.; Chang, C. J. *Curr. Opin. Chem. Biol.* **2010**, 14, 50.

(15) Kim, H. M.; Choo, H. J.; Jung, S. Y.; Ko, Y. G.; Park, W. H.; Jeon, S. J.; Kim, C. H.; Joo, T.; Cho, B. R. *ChemBioChem* **2007**, 8, 553.

(16) *A Guide to Fluorescent Probes and Labeling Technologies*, 10th ed.; Haugland, R. P., Ed.; Molecular Probes: Eugene, OR, 2005.

(17) Hultberg, B.; Andersson, A.; Isaksson, A. *Toxicology* **2002**, 175, 103.

(18) Yellaturu, C. R.; Bhanoori, M.; Neeli, I.; Rao, G. N. *J. Biol. Chem.* **2002**, 277, 40148.